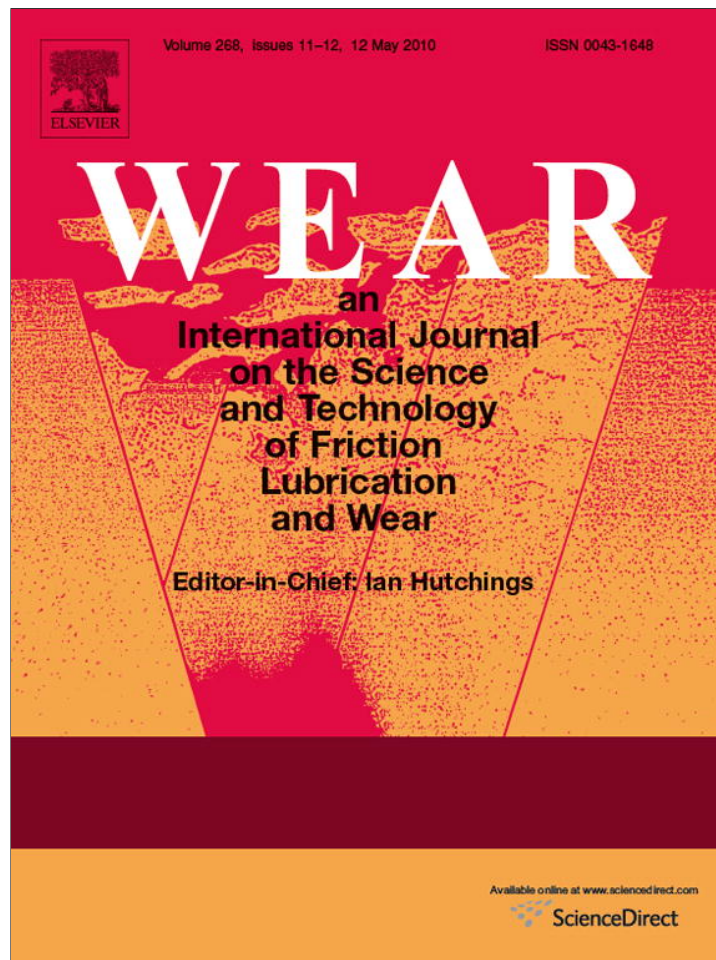


Provided for non-commercial research and education use.  
Not for reproduction, distribution or commercial use.



This article appeared in a journal published by Elsevier. The attached copy is furnished to the author for internal non-commercial research and education use, including for instruction at the authors institution and sharing with colleagues.

Other uses, including reproduction and distribution, or selling or licensing copies, or posting to personal, institutional or third party websites are prohibited.

In most cases authors are permitted to post their version of the article (e.g. in Word or Tex form) to their personal website or institutional repository. Authors requiring further information regarding Elsevier's archiving and manuscript policies are encouraged to visit:

<http://www.elsevier.com/copyright>



# Investigation of fretting wear at the dimple/gimbal interface in a hard disk drive suspension

B. Raeymaekers<sup>a,\*</sup>, S. Helm<sup>a</sup>, R. Brunner<sup>a</sup>, E.B. Fanslau<sup>b</sup>, F.E. Talke<sup>a</sup>

<sup>a</sup> University of California San Diego, 9500 Gilman Dr., La Jolla, CA 92093-0401, United States

<sup>b</sup> NHK International Corp., 2350 Mission College Blvd., Santa Clara, CA 95054, United States

## ARTICLE INFO

### Article history:

Received 12 August 2009

Received in revised form 29 January 2010

Accepted 2 February 2010

Available online 16 February 2010

### Keywords:

Fretting

Hard disk drive

Wear

## ABSTRACT

Fretting wear of the dimple/gimbal interface in a hard disk drive suspension is investigated. The energy dissipated between the dimple and the gimbal spring is determined as a function of operating conditions and material properties, and related to the wear observed at the interface. Abrasive, adhesive and tribochemical wear are found to be present. A thin film of gold on the gimbal resulted in the best wear behavior.

© 2010 Elsevier B.V. All rights reserved.

## 1. Introduction

Decreasing flying height between the magnetic read/write head and the magnetic disk in a hard disk drive makes the head/disk interface more vulnerable to failure as a result of contact between slider and disk. Examination of failed hard disk drives has shown that microscopically small wear particles are likely to be responsible for hard disk drive failure [1].

One source of wear particles in a hard disk drive is fretting wear between the dimple and the gimbal of a hard disk drive suspension. Fig. 1(a) shows a top view of a typical hard disk drive suspension assembly and Fig. 1(b) shows a side view of the suspension assembly. The slider, which contains the magnetic read/write element, is connected to the gimbal spring. The gimbal spring is attached to the suspension. A hemispherical dimple of approximately 200  $\mu\text{m}$  radius is punched in the suspension surface to allow roll and pitch motion of the gimbal with the slider.

During operation of a hard disk drive, the suspension arm positions the slider over the recording tracks. The positioning of the suspension arm over the disk creates a small-amplitude slip motion between the surface of the dimple and the surface of the gimbal spring. This slip motion is highly undesirable since it can cause the formation of wear particles that could lead to failure of the hard disk drive. A similar event in terms of small scale motion and creation of undesirable wear particles occurs also during the load/unload process, during track seeking, during axial motion of the slider due

to disk run-out, as well as during external shocks to which the disk drive is exposed. At present, very little information is present in the open literature concerning the tribology of the gimbal/dimple interface. In this paper we address this gap by studying the wear at the dimple/gimbal interface as a function of material properties and operating conditions.

## 2. Fretting wear

Fretting is defined as a cyclic relative motion between two surfaces in contact at small displacement amplitude [2,3]. Depending on material properties, loading conditions and environment, fretting can cause crack formation or fretting wear [4,5]. Mechanisms for fretting wear are oxidation, adhesion, surface fatigue or abrasion [6]. Experimental investigations have shown that cyclic motion at the contact interface between two bodies can be divided into four different regimes of sliding: stick, partial slip, gross slip and reciprocal sliding [7,8]. A detailed description of the four fretting regimes is provided in Ref. [7]. These different regimes can be characterized as a function of normal load and displacement amplitude using so-called “fretting maps” [7,9].

Varenberg et al. [10] introduced a so-called “slip index”, a criterion to determine different fretting regimes from a friction force versus relative displacement (friction hysteresis loop) measurement of the reciprocal motion between two samples [10,11]. They defined a slip index  $\delta$  as

$$\delta = \frac{A_d S_c}{N} \quad (1)$$

\* Corresponding author. Fax: +1 858 534 2720.

E-mail address: [bart@talkelab.ucsd.edu](mailto:bart@talkelab.ucsd.edu) (B. Raeymaekers).

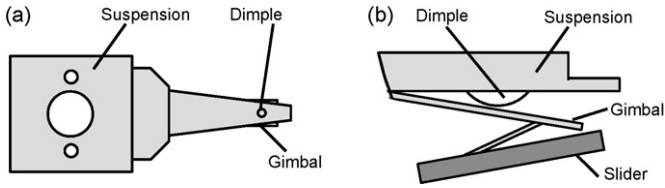


Fig. 1. (a) Top view and (b) side view of suspension assembly.

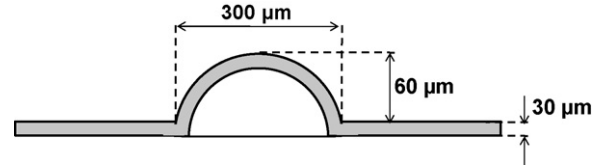


Fig. 4. Cross-sectional view of the dimple.

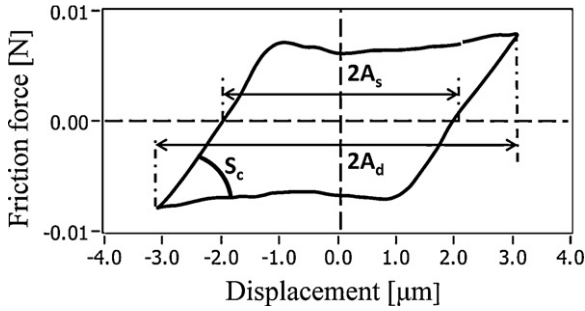


Fig. 2. Friction hysteresis loop definitions.

actuator is driven with a triangularly shaped input voltage signal with constant amplitude. The displacement of the PZT actuator (see Fig. 3(c)) is measured with an optical displacement sensor. The load cell measures the friction force  $F_t$  created between the dimple and the gimbal material, as illustrated in Fig. 3(b). We have verified that the displacement of the suspension due to the friction force acting on the dimple is typically less than 10% of the displacement amplitude of the gimbal. Thus, the error committed in the measurement of the friction hysteresis loops using only one displacement measurement on the gimbal rather than two independent displacement measurements on the gimbal and the dimple, is small in the present study and can be neglected. It should be pointed out, however, that under high frictional load separate measurement of the displacement of both the dimple and the gimbal may be desirable to improve the accuracy of the friction hysteresis loops.

where  $A_d$  is the maximum displacement amplitude,  $S_c$  is the slope of the typical friction hysteresis loop, and  $N$  is the normal load, as illustrated in Fig. 2.  $A_s$  is the slip amplitude.

The transition between the four fretting regimes for a given loading condition can be specified by the slip index, which, according to Varenberg, is universal for any scale from nano- to macro-fretting [11]. Varenberg identified the four regimes of sliding in terms of the slip index. Reciprocal sliding was found to occur when  $\delta > 11$  and fretting was restricted to  $\delta < 10$ . Gross slip was found between  $0.8 < \delta < 10$  and partial slip between  $0.5 < \delta < 0.6$ . The regime  $\delta < 0.5$  was suggested to correspond to stick, pending more experimental validation.

### 3. Experimental apparatus

Fig. 3(a) shows a schematic of the experimental apparatus used in this study. A suspension is attached to a strain gauge based load cell. The suspension is placed adjacent to the gimbal as shown in Fig. 3(b). The dimple of the suspension is loaded against the gimbal material, which is attached to a shear mode piezo (PZT) actuator. The PZT actuator, if energized, causes a reciprocating motion between dimple and gimbal. The normal force  $N$  is applied to the dimple by means of a calibrated dead weight. The shear mode PZT

### 4. Test procedure and samples

In our initial studies, we have used commercially available, stainless steel hard disk drive suspensions. For each test a new suspension was used. Fig. 4 shows the cross-section of the suspension with the typical dimensions of the dimple.

Table 1 summarizes the surface and material properties for the different gimbal and dimple materials used in this investigation. We have selected different materials and coatings to cover a wide range of material and surface properties. The Young's modulus  $E$  was taken from the literature and the hardness  $H$  was measured using a nano-indenter. The thickness of the coatings is on the order of several micrometers. The surface roughness was measured using an atomic force microscope. The measurements showed that the surface roughness of the dimple and gimbal is isotropic. Hence, the Greenwood–Williamson approach can be used to describe the surface roughness of gimbal and dimple [12]. The average asperity tip radius  $\rho$ , the asperity density  $\eta$ , and the standard deviation of asperity summit heights  $\sigma_s$  can be obtained using the three spectral moments  $m_0$ ,  $m_2$ , and  $m_4$  of the surface roughness as described by McCool [13] (see Appendix A);  $\sigma_s/\rho$  is a measure for the surface roughness. A low value (high  $\rho$  and low  $\sigma_s$ ) indicates a smooth surface, and vice versa.

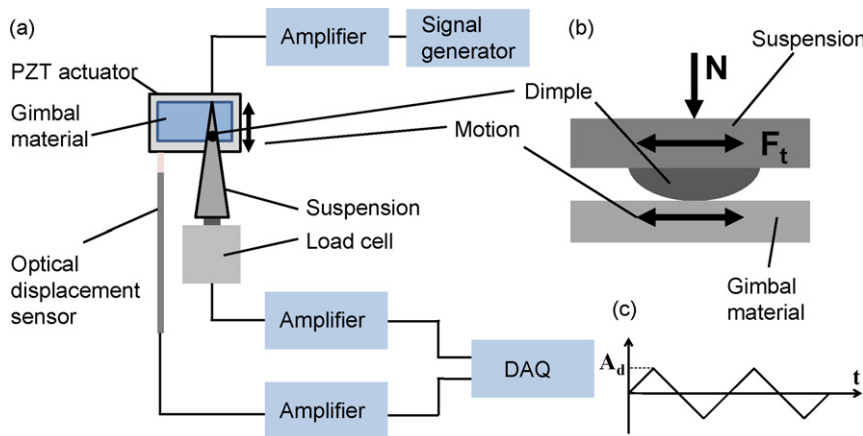


Fig. 3. (a) Schematic of experimental set-up and (b) detailed side view of dimple/gimbal interface.

**Table 1**  
Material samples properties (before experiment).

Code	Material	$\rho$ (nm)	$\eta$ (nm <sup>-2</sup> )	$\sigma_s$ (nm)	$\sigma_s/\rho$	$E$ (GPa)	$H$ (GPa)
G1	Stainless steel	6450.19	3.52E-07	42.86	6.64E-03	200.00	3.70
G2	Stainless steel	6253.11	2.85E-07	43.37	6.94E-03	200.00	4.70
G3	Nickel-coated	30026.43	1.57E-07	28.96	9.64E-04	200.00	4.49
G4	Gold-coated	3494.95	1.28E-06	10.75	3.08E-03	80.00	0.36
D1	Stainless steel	3314.42	1.02E-06	41.53	1.25E-02	200.00	3.92
D2	Laser polished stainless steel	78824.29	3.01E-08	28.39	3.60E-04	200.00	3.62
D3	Copper-coated	11740.92	1.62E-06	11.65	9.92E-04	130.00	1.06
D4	SiN-coated	6695.69	4.09E-07	33.55	5.01E-03	160.00	2.57

**Table 2**  
Material sample combinations surface properties (before experiment).

Combination	$\rho$ (nm)	$\eta$ (nm <sup>-2</sup> )	$\sigma_s$ (nm)	$\sigma_s/\rho$
D1/G1	2948.00	7.32E-07	59.89	2.03E-02
D1/G2	2928.48	6.53E-07	60.44	2.06E-02
D1/G3	3294.41	9.59E-07	50.75	1.54E-02
D1/G4	2404.94	1.13E-06	42.91	1.78E-02
D2/G1	6428.71	3.29E-07	51.94	8.08E-03
D3/G1	5653.25	4.30E-07	44.53	7.88E-03
D4/G1	4645.34	3.77E-07	54.44	1.17E-02

From Table 1 we note that G3, D2 and D3 are the smoothest surfaces (lowest  $\sigma_s/\rho$ ). G2, G3 and D1 are the hardest materials of all samples under investigation. Table 2 shows the equivalent surface roughness parameters for two contacting rough surfaces [13].

From Table 2, D2/G1 and D3/G1 yield the lowest equivalent surface roughness of all material combinations we have tested.

Each experiment was conducted five times and the results were averaged over all experiments. We have used discrete frequencies of 1, 2 and 5 Hz for the reciprocating motion of the gimbal material, with an amplitude  $A_d = 3 \mu\text{m}$ . A normal load was applied to the suspension by adding a calibrated weight to the suspension surface, directly over the dimple. We have used normal forces ranging between 10 and 50 mN. Typical hard disk drive suspensions operate with a normal load between 20 and 30 mN.

**5. Results**

Fig. 5 shows the slip index as a function of the number of fretting cycles for different normal loads, for a stainless steel dimple D1 against a stainless steel gimbal G1 (see Table 1). This combination of stainless steel dimple versus stainless steel gimbal (D1/G1) serves as benchmark throughout this paper, since it represents the typical case in a hard disk drive of a stainless steel dimple on a stainless steel gimbal, without lubrication. The dashed horizontal line at

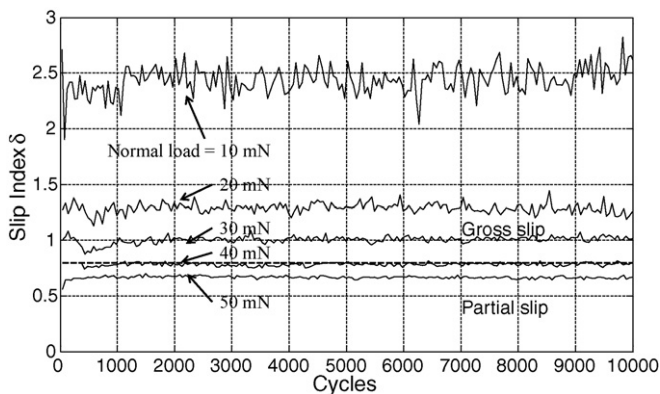


**Fig. 5.** Slip index versus number of cycles (D1/G1).

$\delta = 0.8$  represents the transition from the gross slip to the partial slip regime. From Fig. 5 we observe that the slip index remains approximately constant over all 10,000 cycles, i.e., the fretting regime remains invariable during the experiment. Based on this result it is justifiable to use the average slip index over all fretting cycles of one experiment when comparing different experiments with each other.

Fig. 6 shows the slip index versus the normal load for frequencies of 1, 2, and 5 Hz for a stainless steel dimple versus a stainless steel gimbal (D1/G1). We observe that the slip index decreases with increasing normal load, and that it is almost independent of frequency within the range of our experiment. A horizontal dashed line at a slip index value of  $\delta = 0.8$  indicates the transition from gross slip to partial slip, which, in our experiment, seems to occur at a normal load of approximately 40 mN. Fig. 7 shows typical friction hysteresis loops, i.e., friction force versus relative displacement, for normal loads of 10, 20 and 50 mN. We observe that the slip amplitude  $A_s$  decreases with increasing normal load. Very little slip occurs at a normal load of 50 mN. Clearly, almost no energy is dissipated in this case since the area within the hysteresis loop is almost zero. It has been shown by Fouvry et al. [14,15], and Yu et al. [16] that the dissipated energy during one fretting cycle is related to the wear produced during that cycle. Optical microscopy images (Fig. 7) provide an estimate of the shape and magnitude of the wear scar created by the fretting experiment on the dimple. From Fig. 7 we observe that the size of the wear scar increases if the load is increased from 10 to 20 mN. However, as the load is increased further, to 50 mN, the size of the wear scar decreases.

Fig. 8 shows the wear scars that were created on the gimbal material as a result of the fretting experiment. From Fig. 8 we observe the same trend as from Fig. 7; the size of the wear scar on the gimbal increases if the load is increased from 10 to 20 mN. However, as the load is increased further, to 50 mN, the size of the wear scar decreases.

Fig. 9 shows the dissipated energy as a function of the normal load, for frequencies of 1, 2 and 5 Hz. We observe that the energy dissipation in the case of a 20 mN normal load is higher than in the case of a load of 10 or 50 mN. At normal loads of 10–20 mN, the

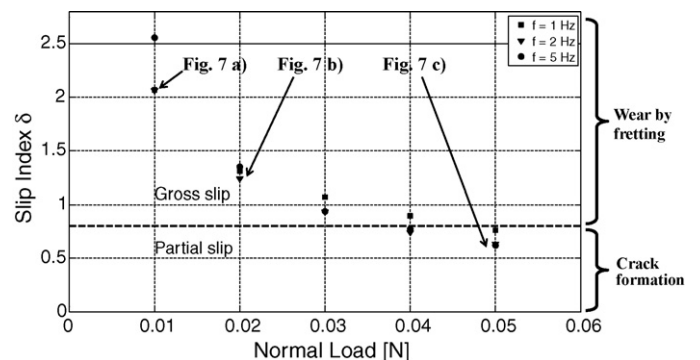


**Fig. 6.** Slip index versus normal load (D1/G1) for 1, 2 and 5 Hz.

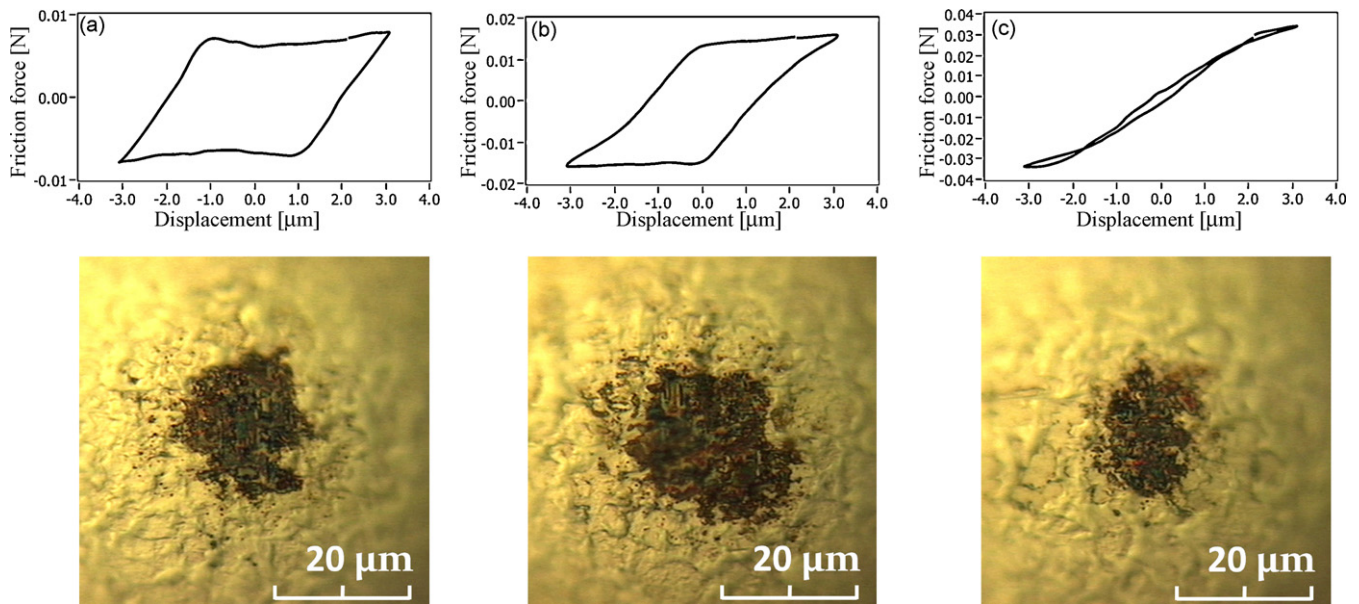


Fig. 7. Friction hysteresis loop and wear scar on the dimple (D1/G1) after 10,000 cycles with  $f=1$  Hz, for a normal load (a)  $N=10$  mN, (b)  $N=20$  mN and (c)  $N=50$  mN.

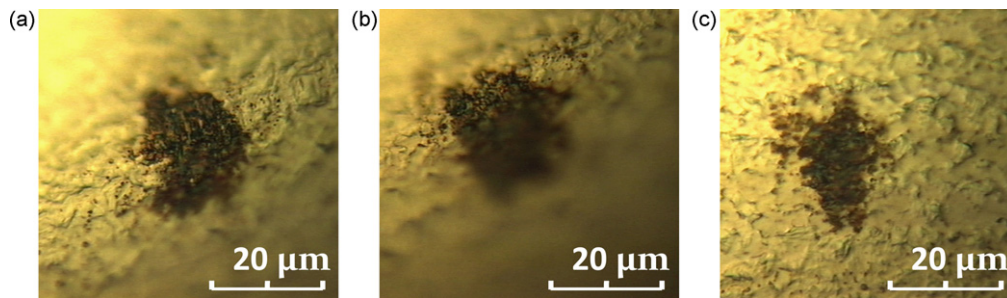


Fig. 8. Wear scar on the gimbal (D1/G1) after 10,000 cycles with  $f=1$  Hz, for a normal load (a)  $N=10$  mN, (b)  $N=20$  mN and (c)  $N=50$  mN.

dimple/gimbal interface operates in the gross slip regime, i.e., the entire dimple is sliding over the gimbal. When the normal load increases, the contact area between the dimple and the gimbal increases, and, thus, more wear occurs. Simultaneously, the sliding amplitude reduces with increasing normal load. Thus, starting from a normal load of 40 mN, fretting changes from gross slip to partial slip (see Fig. 6). Therefore, less energy will be dissipated, and, accordingly, less wear will be produced. From Fig. 9 we also notice that the effect of frequency on dissipated energy, within the range of frequencies tested, is small.

Fig. 10 shows the slip index as a function of normal load, for different gimbal materials (stainless steel, nickel-coated stainless steel, gold). The frequency of the reciprocating motion was chosen to be 1 Hz. We observe that the slip index for D1/G1, D1/G2, and D1/G3 is very similar, and that the gold-coated gimbal results in the lowest slip index.

Fig. 11 shows the dissipated energy as a function of normal load after 10,000 cycles ( $f=1$  Hz), for the following gimbal materials: stainless steel, Ni-coated, and gold-coated (3  $\mu$ m). Similar to Fig. 9 we observe a maximum around 20–30 mN regardless of the

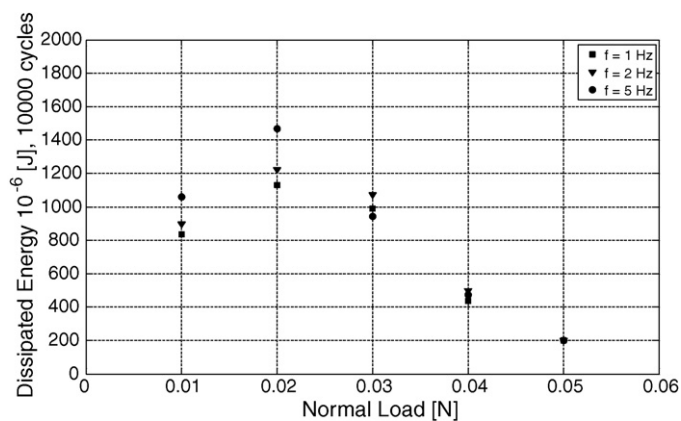


Fig. 9. Dissipated energy versus normal load (D1/G1).

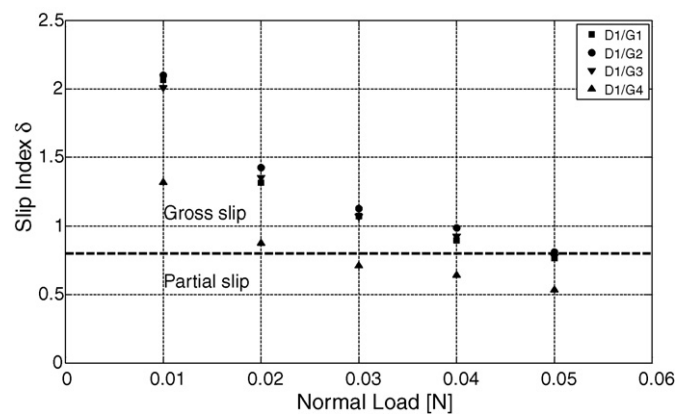


Fig. 10. Slip index versus normal load for different gimbal materials,  $f=1$  Hz.

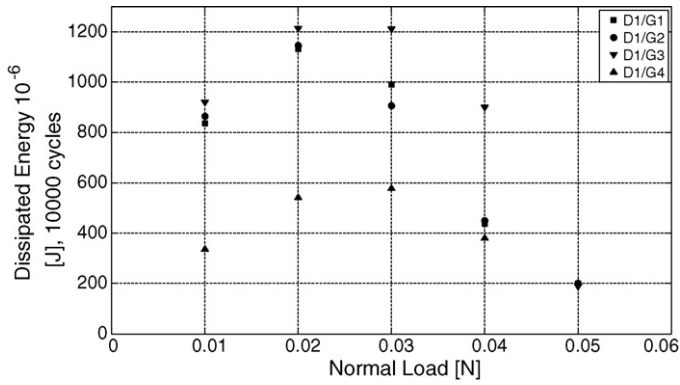


Fig. 11. Dissipated energy versus normal load for different gimbal materials,  $f=1$  Hz.

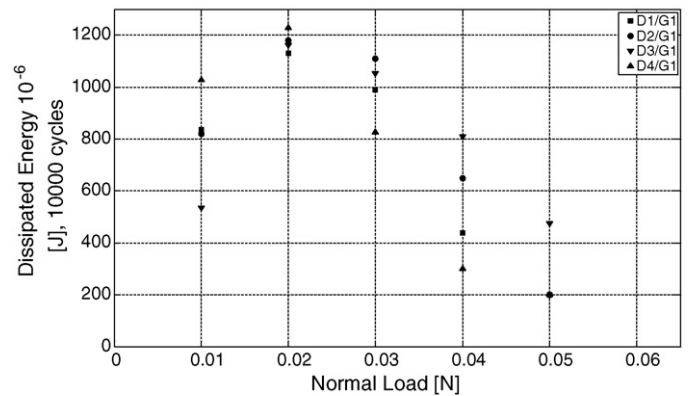


Fig. 13. Dissipated energy versus normal load for different dimple materials,  $f=1$  Hz.

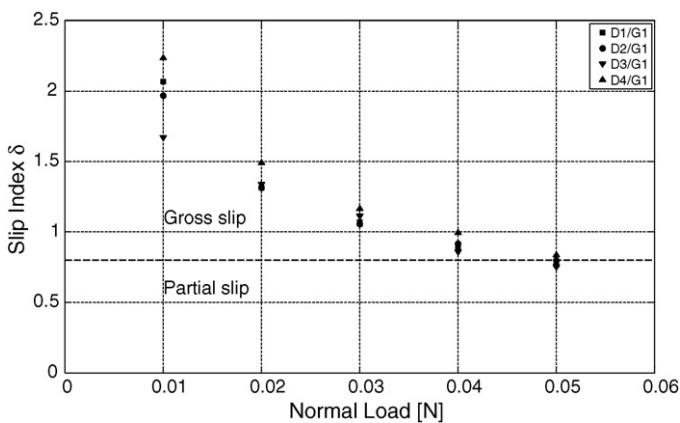


Fig. 12. Slip index versus normal load for different dimple materials,  $f=1$  Hz.

combination of materials used. Less dissipated energy indicates a smaller amount of wear for a particular material combination. We observe that less than half of the energy was dissipated during the experiments with the gold-coated gimbal (D1/G4) compared to the experiments with the stainless steel gimbal materials (D1/G1 and D1/G2), and the nickel-coated surface (D1/G3). Since the relationship between dissipated energy and wear is different for each material combination, it is not possible to directly relate wear to dissipated energy for different material pairs. Additionally, when analyzing the wear scar on the dimples with energy dispersive X-ray spectroscopy (EDX), no gold transfer from the gimbal to the dimple was observed.

Fig. 12 shows the slip index as a function of normal load for the following dimple materials: stainless steel, laser polished stainless steel, Cu-coated stainless steel and SiN-coated stainless steel. The SiN-coated dimple yields the highest slip index for a particular normal load, while the Cu-coated dimple yields the lowest slip index. However, we observe that with increasing nor-

mal load, the slip index becomes very similar for all materials used.

Fig. 13 shows the dissipated energy as a function of normal load after 10,000 cycles, for the same materials as shown in Fig. 12. We observe that the dissipated energy after 10,000 cycles follows the same pattern as observed in Fig. 9. The maximum energy dissipation occurs at a 20 mN load, regardless of the materials used. At a normal load of 10 mN the copper-coated dimple (D3/G1) shows the lowest energy dissipation, while at 40 mN the SiN-coated dimple (D4/G1) results in the lowest energy dissipation.

For a dimple coated with Cu or SiN “flaking” of the coating was generally observed after 10k cycles, while the gold-coated gimbal remained clean and smooth. A set of typical optical microscopy images is shown in Fig. 13 for (a) a gold-coated gimbal (D1/G4), (b) a copper-coated dimple (D3/G1) and (c) a SiN-coated dimple (D4/G1) after 10,000 cycles ( $f=1$  Hz and  $N=30$  mN). Similar to Fig. 11 it is not possible to directly relate wear to dissipated energy for different material pairs.

From Fig. 14 we observe that the coatings on the dimple (Fig. 14(b) and (c)) showed substantial discoloration and damage due to flaking and oxidation, while the gold coating (Fig. 14(a)) on the gimbal remained intact. Slight signs of plastic deformation are visible on the gold gimbal.

## 6. Discussion

The results for wear of the dimple/gimbal interface have shown substantial differences as a function of material properties and experimental conditions. A number of ways exist to reduce wear and wear particle formation. In particular, based on the data it appears reasonable to suggest that an increase in normal load applied to the suspension would reduce fretting, and therefore, reduce the formation of wear particles. In terms of fretting wear characteristics, an increase in the normal load from 20 mN to 40 or

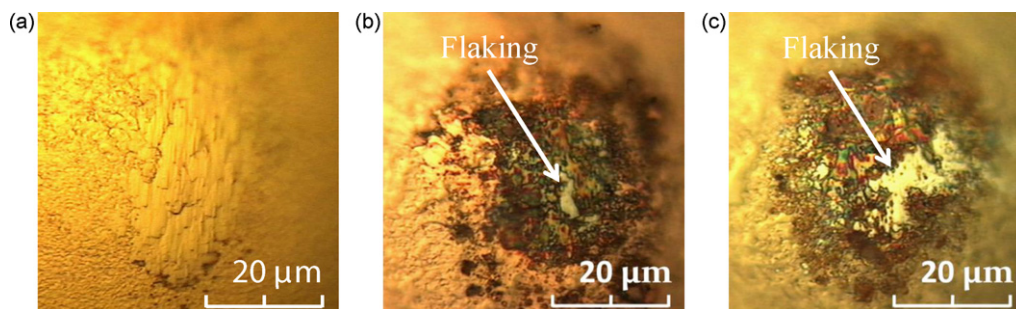


Fig. 14. Optical microscope images of (a) a gold-coated gimbal (D1/G4), (b) a copper-coated dimple (D3/G1) and (c) a SiN-coated dimple (D4/G1),  $f=1$  Hz and  $N=30$  mN.

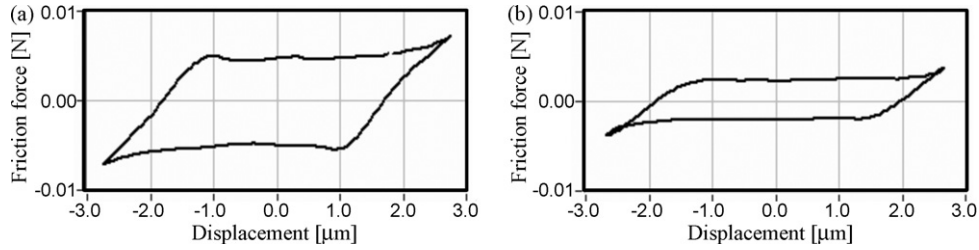


Fig. 15. Friction hysteresis loop for (a) D1/G1 and (b) D1/G4 with  $N = 10$  mN.

Table 3  
Plasticity index.

	D1/G1	D1/G2	D1/G3	D1/G4	D2/G1	D3/G1	D4/G1
$\psi_{\text{before}}$	4.67	4.44	3.91	26.38	3.08	8.00	4.54
$\psi_{\text{after}}$	3.50	2.52	2.16	24.05	3.39	10.34	4.62
$d$ ( $\mu\text{m}$ )	30	35	40	10	40	25	40

50 mN would bring the interface in the partial slip fretting regime, which is characterized by less fretting wear. However, an increase in the normal load of the dimple/gimbal interface affects the flying characteristics of the head/disk interface and the shock resistance of the hard disk drive. Hence, an increase in the dimple/gimbal preload is not a realistic option. Another theoretical solution to reduce fretting would be to reduce the tangential stiffness of the dimple/gimbal interface. This could be obtained by choosing a material with a low Young's modulus for the suspension and the gimbal spring.

The fretting experiments for the stainless steel/gold dimple gimbal combination (D1/G4) show the lowest values for the slip index compared to all other materials combinations studied. Fig. 15 shows typical friction hysteresis loops for the stainless steel/stainless steel interface (D1/G1), the stainless steel/gold interface (D1/G4) for a constant normal load and displacement amplitude ( $N = 10$  mN;  $A_d = 3$   $\mu\text{m}$ ). We observe that the slope  $S_c$  of the hysteresis loop is shallower for the stainless steel/gold interface compared to the stainless steel/stainless steel interface. This results in a low value of the slip index (Eq. (1)), yet a high value of the slip ratio  $A_s/A_d$ , as observed in the experiments.

The plasticity index  $\psi$  is an important parameter to characterize elastic-plastic contacts, and is defined as [12]

$$\psi = \frac{2E}{\pi KH} \sqrt{\frac{\sigma_s}{\rho}} \quad (2)$$

where  $\sigma_s$  is the standard deviation of asperity summit heights and  $\rho$  is the mean asperity radius (equivalent value for the combination of two rough surfaces).  $H$  is the hardness of the softer material, and the equivalent Young's modulus  $E$  can be determined from

$$\frac{1}{E} = \frac{1 - \nu_1^2}{E_1} + \frac{1 - \nu_2^2}{E_2} \quad (3)$$

where  $E_1, E_2, \nu_1$  and  $\nu_2$  are the Young's moduli and Poisson's coefficients for both dimple and gimbal material in contact, respectively.  $K$  is a hardness parameter, which is related to the Poisson coefficient of the softer material, and is given as

$$K = 0.454 + 0.41\nu \quad (4)$$

The plasticity index is a function of surfaces roughness and hardness. It changes as a function of the number of fretting cycles. Table 3 compares the plasticity index for all investigated dimple/gimbal combinations before ( $\psi_{\text{before}}$ ) and after ( $\psi_{\text{after}}$ ) a fretting wear test (10,000 cycles,  $f = 1$  Hz,  $N = 30$  mN,  $A_d = 3$   $\mu\text{m}$ ). We observe that the plasticity index is reduced or stays constant for most of the tests, indicating that the surface roughness of the inter-

face decreases for most of the tests, except for the D2/G1, D3/G1 and D4/G1 case, where the surface roughness increased during the experiment. The diameter of the wear scar  $d$  on the dimple, obtained with an optical microscope, is also shown.

Comparing Table 3 with Fig. 11, we conclude that the plasticity index is a very good indicator for the dissipated energy during the fretting experiments. Additionally, the diameter  $d$  of the wear scar on the dimple, was found to be inversely proportional to the plasticity index before the experiment. We notice that in the case of the stainless steel/gold interface the highest plasticity index corresponds to the lowest dissipated energy. The same relationship exists between Fig. 13 and Table 3. We are particularly interested in the relative comparison between the values of the plasticity index rather than evaluating absolute values. The plasticity index contains both surface roughness parameters and material properties, and, thus, allows us to predict the fretting wear resistance of a given pair of sliding bodies. We point out that these results may not be true in general, but only occur in systems with low tangential rigidity such as the dimple/gimbal interface.

## 7. Conclusion

Based on our experiments, we have found that

- (1) Fretting wear between a hemispherical dimple on a hard disk drive suspension and a gimbal spring is highly dependent on the normal load. Decreasing the normal load reduces the contact area and the friction force, and, thus, the wear volume. Increasing the normal load will cause the dimple/gimbal interface to operate in the partial slip fretting regime, which reduces the wear at the dimple/gimbal interface.
- (2) The wear volume is a function of the materials and coatings used for the dimple and gimbal. The plasticity index of the interacting surfaces was found to be a good measure for resistance to fretting wear, with a higher plasticity index implying better wear resistance.
- (3) The combination of a gold-coated gimbal with a stainless steel dimple resulted in the least amount of energy dissipation, which is related to the wear volume.

## Acknowledgements

We wish to thank Hanya-san of NHK international for supporting this research. We would also like to thank Professor Izhak Etsion, and Dr. Andrey Ovcharenko for their interest in this work, and for insightful comments, and Dr. Melanie Gauvin for their help with deposition of some of the thin films used in this study.

## Appendix A.

According to McCool's analysis [13], the spectral moments of a rough isotropic surface are given by

$$m_0 = \text{AVG} [y^2]$$

$$m_2 = \text{AVG} \left[ \left( \frac{dy}{dx} \right)^2 \right]$$

$$m_4 = \text{AVG} \left[ \left( \frac{d^2y}{dx^2} \right)^2 \right]$$

where  $y(x)$  is the height distribution of the surface profile.

The radius of curvature of asperity heights, the areal density of the asperities and the standard deviation of asperity summit heights can be calculated as

$$r = 0.375 \left( \frac{\pi}{m_4} \right)^{1/2}$$

$$\eta = \frac{m_4}{6\pi\sqrt{3}m_2}$$

$$\sigma_s = \left( m_0 - \frac{3.717 \times 10^{-4}}{\eta^2 r^2} \right)^{1/2}$$

For the case of two contacting isotropic rough surfaces 1 and 2, an equivalent rough surface in contact with a smooth flat can be defined. The spectral moments of this equivalent rough surface are given by summing the spectral moments of the individual surfaces. Hence,

$$m_i = (m_i)_1 + (m_i)_2$$

where  $i=0, 2, 4$ .

## References

- [1] D.Y. Lee, J. Hwang, G.N. Bae, Effect of disk rotational speed on contamination particles generated, *Microsyst. Technol.* 10 (2004) 103–108.
- [2] R.B. Waterhouse, *Fretting Corrosion*, Pergamon, Oxford, 1972.
- [3] I.-M. Feng, B.G. Rightmire, The mechanism of fretting, *Lubric. Eng.* 9 (1953) 134–136, and 158–161.
- [4] Y. Berthier, L. Vincent, M. Godet, Fretting fatigue and fretting wear, *Tribol. Int.* 22 (1989) 235–242.
- [5] P.L. Hurricks, The mechanism of fretting—a review, *Wear* 15 (1970) 389–409.
- [6] W.E. Campbell, The current status of fretting corrosion, in: *Symp. Fretting Corrosion*, vol. 4, ASTM Spec. Techn. Publ., 1953, p. 3.
- [7] O. Vingsbo, S. Soderberg, On fretting maps, *Wear* 126 (1988) 131–147.
- [8] S. Fouvry, P. Kapsa, L. Vincent, Analysis of sliding behavior for fretting loadings: determination of transition criteria, *Wear* 185 (1995) 35–46.
- [9] G.X. Chen, Z.R. Zhou, Study on transition between fretting and reciprocating sliding wear, *Wear* 250 (2001) 665–672.
- [10] M. Varenberg, I. Etsion, G. Halperin, Slip index: a new unified approach to fretting, *Tribol. Lett.* 17 (3) (2004) 569–573.
- [11] M. Varenberg, I. Etsion, G. Halperin, Nanoscale fretting wear study by scanning probe microscopy, *Tribol. Lett.* 18 (2005) 493–498.
- [12] J.A. Greenwood, J.B.P. Williamson, Contact of nominally flat surfaces, *Proc. R. Soc. Lond., Ser. A* 295 (1966) 300–319.
- [13] J.I. McCool, Relating profile instrument measurements to the functional performance of rough surfaces, *J. Tribol. Trans. ASME* 109 (1987) 264.
- [14] S. Fouvry, P. Kapsa, L. Vincent, Quantification of fretting damage, *Wear* 200 (1996) 186–205.
- [15] S. Fouvry, C. Paulin, S. Deyber, Impact of contact size and gross-partial slip conditions on Ti-6Al-4V/Ti-6Al-4V fretting wear, *Tribol. Int.* 42 (2009) 461–474.
- [16] J. Yu, L. Qian, B. Yu, Z. Zhou, Nanofretting behavior of monocrystalline silicon (100) against SiO<sub>2</sub> microsphere in vacuum, *Tribol. Lett.* 34 (2009) 31–40.